J Mater Sci (2011) 46:6812–6822
DOI 10.1007/s10853-011-5640-3

Methods for enhanced control over the density and electrical properties of SWNT networks

L. David Lipscomb · Pornnipa Vichchulada · Nidhi P. Bhatt · Qinghui Zhang · Marcus D. Lay

Received: 15 March 2011 / Accepted: 16 May 2011 / Published online: 1 June 2011

Abstract The formation of manufacturable electronic materials that incorporate single-walled carbon nanotubes (SWNTs) will most likely involve the use of networks of these molecular wires, due to the enhanced current drive and reproducibility of such films. Therefore, control over the density of SWNTs during the deposition of 2-D networks is of critical importance for the development of numerous enhanced electronic materials. Room temperature deposition methods are of particular interest as they allow separation, purification, and/or chemical modification of SWNTs before deposition. This article reports three iterative liquid-deposition techniques that allow control over the properties of three distinct types of SWNT networks. First, density control was obtained for 2-D networks of unbundled, high-aspect ratio SWNTs. Such networks exhibited semiconductive behavior, with tunable on/off ratios. Second, electrically continuous 2-D clusters of high aspect ratio SWNTs were formed by allowing capillary forces to develop in a sessile suspension droplet. These constructs displayed tunable metallic conductivity, and may have the applications as interconnects in microelectronics. Finally, highly conductive, 3-D networks of bundled SWNTs were formed via an evaporation method. For these three types of networks, the density of SWNTs, and thus the macroscopic conductance, was readily controlled via the number of deposition cycles used in their formation.

L. D. Lipscomb · P. Vichchulada · N. P. Bhatt · Q. Zhang · M. D. Lay (✉)
Department of Chemistry, Center for Nanoscale Electronic Materials (CNEM), University of Georgia, Athens, GA 30602, USA
e-mail: mlay@uga.edu

Introduction

Single-walled carbon nanotubes (SWNTs) have unique electrical properties that are useful in a variety of electronic device structures. Therefore, they have been investigated for use as quantum wires [1], field-effect transistors (FETs) [2], and current-rectifying diodes [3]. However, device structures based on individual nanotubes are impractical because of their low current drive relative to that of conventional Si-based electronic materials [4, 5], variations in the electrical properties of SWNTs [6], and significant manufacturing difficulties with regard to scale-up [7, 8].

The most promising route to the formation of reproducible SWNT-based device structures is the use of thin-films of electrically continuous networks [9–11]. Such arrays exhibit greater tunability and reproducibility, as the SWNT density is the major determining factor for the macroscopic electrical properties [10, 12]. These networks behave as semiconductive thin-films when composed of low densities of unbundled SWNTs. When SWNTs are bundled together and/or in high-density networks, the material exhibits metallic conduction, with conductivity increasing commensurate with SWNT density. Both types of networks have a much higher current drive than an individual SWNT, as the current load is directly proportional to the number of SWNTs in the network. Further, networks can be fabricated with much greater inter-device precision and can be more easily combined with existing industrial micro-fabrication methods. Therefore, SWNT networks are being investigated for numerous applications, including light-weight flexible displays [13–15], nanocomposites for energy storage [16], supercapacitors [17], and sensors [18, 19].

Room-temperature routes to SWNT network formation will allow the creation of new lightweight, energy efficient

electronic materials. In particular, liquid deposition methods are of significant interest as they allow the incorporation of purification and/or chemical modification steps before network formation [20, 21]. Previously reported liquid deposition approaches include SWNT network deposition using filtration [22], printing [23, 24], dip-coating [25], spray-coating [26], and laminar fluid-flow methods [27, 28].

As networks of bundled [3, 29] and unbundled [30, 31] SWNTs have very different properties and applications, there is a great necessity for the development of deposition methods that allow control over the density and degree of bundle formation of nanotubes in the network. For the networks described in this manuscript, a new purification method for the formation of suspensions of unbundled, high aspect ratio SWNTs was used to ensure that any bundles observed in deposits occurred as a result of the deposition method [32]. Then, three approaches to the development of methods for maintaining density control throughout the formation of SWNT networks were investigated. First, low-density, 2-D networks of unbundled SWNTs were formed via a repeated deposition process that reproducibly deposited arbitrary densities of SWNTs (painted-spin, PS). Second, 2-D clusters of SWNTs were formed by combining a previously reported SWNT purification process for the production of high aspect ratio SWNTs [20] with the "coffee-ring" deposition phenomenon (incubated-spin, IS); [33] these high-aspect ratio SWNTs behaved uniquely when deposited from sessile aqueous droplets. Finally, high-density, 3-D networks of high-aspect ratio SWNTs were formed via a repeated evaporation method (coated-dry, CD).

Experimental

Preparation and characterization methods

SWNT suspension preparation

As SWNTs aggregate during the growth process due to strong Van der Waals interactions, a new method of forming suspensions of unbundled, high-aspect ratio SWNTs was used [32]. In brief, low power probe sonication (Branson, Model 250) was employed to unbundle the SWNTs while minimizing sonication-induced damage. Next, repeated centrifugation (45 min at 18,000$\times g$, Beckman, GS-15R) and decantation cycles were employed to form stable suspensions enriched in high-aspect ratio SWNTs. The purified suspensions utilized for depositing the networks were composed of 0.02 mg/mL arc discharge SWNTs (Carbolex, AP-grade) in 1% w/v sodium dodecyl sulfate (SDS), with the exception of one concentrated suspension (0.1 mg/mL) that was employed to deposit an ultra-low density of SWNTs for the PS electrical characterization studies, as described below. All suspensions were evaluated with UV–Vis–NIR spectroscopy (Agilent, Cary 5000) before network formation.

The presence of unbundled SWNTs in a suspension can be verified with UV–Vis–NIR spectroscopy [34, 35]. Spectra for suspensions of unbundled SWNTs have enhanced peaks indicative of interband transitions for metallic (M_{11}, 400–650 nm) and semiconductive SWNTs (S_{22}, 550–900 nm and S_{11}, 900–1600 nm). These transitions are diminished in suspensions of bundled SWNTs (Fig. 1a). In addition, the high absorbance observed for unpurified suspensions is due to the presence of carbonaceous impurities as well as bundles of SWNTs. In contrast, spectra for purified suspensions show enhanced absorbance peaks due to interband transitions in unbundled SWNTs (Fig. 1b). Therefore, as the suspensions are composed of unbundled SWNTs (as confirmed with AFM as well), the challenge becomes determining the effect of the deposition method on the formation of bundles in each deposit.

The formation of suspensions of unbundled SWNTs is crucial to the formation of electronic materials, as individual SWNTs have a 2/3rd probability of being semiconductive and 1/3rd probability of being metallic [36–38]. This property allows low-density networks of unbundled SWNTs to behave as semiconductive thin films, while bundles of SWNTs behave as metallic conductors. Previous semiconductor device characterization studies of deposits formed from untreated and purified suspensions have shown the effectiveness of this purification method for the formation of unbundled deposits [39]. Owing to the presence of SWNT bundles and other impurities, little gating was observed for untreated suspensions, while suspensions of unbundled SWNTs could be utilized to form transistors, the conductance of which could be effected by the application of a gate bias.

Substrate preparation

Silicon wafers, with a 300 nm thermally grown oxide layer, were cleaned with a CO_2 "snow-jet" before and after the deposition of a monolayer of (3-aminopropyl) triethoxysilane (Sigma-Aldrich) [40]. This monolayer acted as an adhesion layer. An enamel-based copolymer acrylate was used as a mask during the silanization process to confine the silane to a square area between the source/drain electrode pairs. These electrodes were composed of 150 nm of Ti deposited through a stencil using a thermal evaporator (Thermionics).

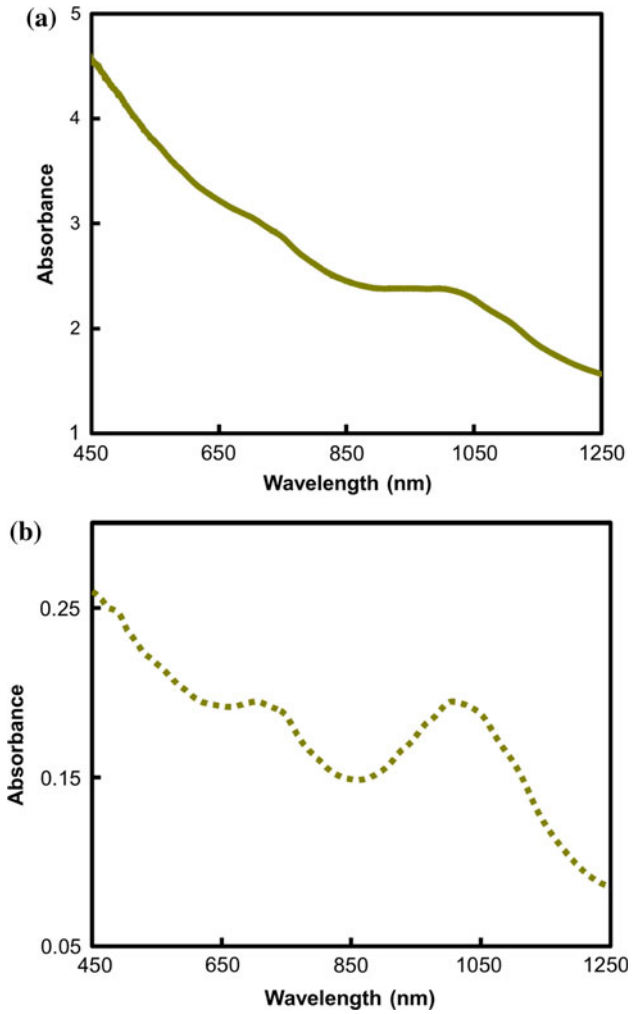

Fig. 1 **a** UV–Vis–NIR spectroscopy of suspensions showed a high absorbance and relatively small interband transitions, as typically observed for suspensions of bundled SWNTs, while **b** the reduced absorbance and enhanced peaks corresponding to interband transitions in unbundled SWNTs confirms the ability to transform the suspensions of bundled SWNTs into stable suspensions of unbundles SWNTs used in these studies

SWNT network characterization techniques

In order to quantify the effect of each deposition method on the resulting SWNT network morphology, deposits formed using each method were examined with intermittent mode atomic force microscopy (AFM, Pico Plus, Molecular Imaging). A minimum of five representative images, from the center, halfway point, and edge of the network were obtained for each method following each deposition cycle. Height histograms for the AFM images were generated with image analysis software (SPIP v.5.1, Imagemet).

A probe station and a semiconductor characterization (Signatone, S-1160 and Keithley, 4200, respectively) unit were used for electrical characterization of devices. Two-point probe resistance measurements were obtained by contacting prefabricated Ti electrodes and generating an *I/V* curve for each sample after each deposition cycle. A two-point probe method was advantageous in these studies, as it allowed a direct comparison of the change in resistance for each type of device, while also allowing the determination of its on/off ratio via a standard three-terminal semiconductor device characterization setup.

Liquid deposition methods for SWNT network formation

An iterative deposition method, that involved alternating deposition and rinse cycles, was applied to a rotating Si/SiO_x wafer that was mounted on a spin-coater (Laurell Technologies, WS-400). For rinse cycles, 25 mL of 65 °C nanopure-H_2O was applied at the rate of 1 mL/s as the substrate spun at 5,500 rpm. The three spin casting methods are denoted painted-spin (PS), incubated-spin (IS) and coated-dry (CD).

PS method

400 μL of SWNT suspension was drop-cast onto the rotational center of a 2″ Si/SiO_x wafer. Next, the sample was spun at a rate of 60 rpm, as the suspension was painted from the center to the edge of the wafer at a rate of 0.5 cm/s. Then, the spin rate was rapidly accelerated up to 1500 rpm, where it remained for 45 s. Finally, a rinse cycle was applied to the substrate. This deposition/rinse cycle was repeated to tune the macroscopic conductivity of these networks. In addition to minimizing waste, this procedure was the most effective for eliminating bundle formation during SWNT network deposition, resulting in a uniform network over the entire wafer.

IS method

4 mL of SWNT suspension was drop-cast onto the center of the substrate. After an incubation time of 10–12 min, the sample was spun at 1200 rpm for 45 s. This deposition period was followed by a rinse stage. As deposition of SWNTs occurred preferentially at the drop's edge, as described in detail below, this process was repeated with successively larger volumes of suspension to produce a network with macroscopic conductance.

CD method

4 mL of SWNT suspension was drop-cast onto a wafer and spread to coat the entire surface. After complete drying, the sample was rinsed. This process was repeated to increase the conductivity of the deposited SWNT thin film.

Results and discussion

As-produced (AP) grade arc discharge soot contains bundles, or ropes, composed of 50–100 SWNTs held together by relatively strong van der Waals attractions. As the suspension preparation method used for these studies has proven effective for the formation of stable suspensions of unbundled, high-aspect ratio SWNTs [20], the effect of each deposition method on bundle formation could be ascertained from the analysis of AFM images of the deposits. For the PS deposition method, less than 10% of tubes observed had heights greater than 2.0 nm, indicating the deposition of unbundled SWNTs. The ability of this deposition method to form deposits that exhibited FET behavior, further confirmed the formation of low-density networks of unbundled SWNTs. Therefore, the bundles observed in the IS and CD methods were not present in the suspension, but likely formed during the deposition process.

Effect of deposition method on network morphology and surface roughness

PS method

SWNT networks formed using the PS method had the lowest density of bundles, as observed via AFM, with the density of randomly oriented SWNTs increasing reproducibly from one deposition cycle to the next (Fig. 2). The density of these networks could be tuned via either the number of deposition cycles, or changing the concentration of SWNTs in the deposition suspension. For the deposition

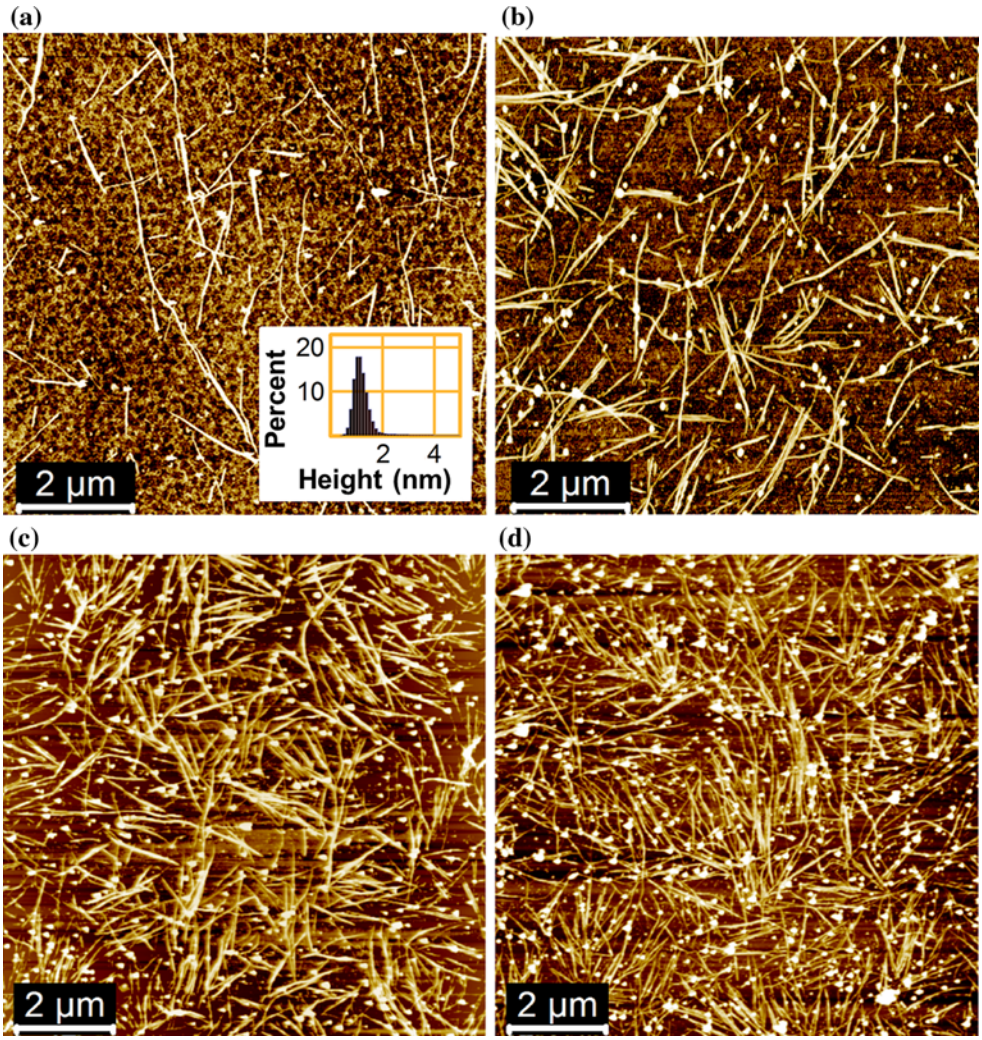

Fig. 2 Networks composed of spin-cast high-aspect ratio SWNTs using the PS method **a** five deposition cycles resulted in a sparse network that does not exhibit macroscopic conductivity; **b** 10 deposition cycles increases the density of SWNTs above the percolation threshold for semiconductive SWNTs; **c** 12 deposition cycles results in a deposit with increasing metallic behavior; **d** 25 deposition cycles further increases sheet conductance

Table 1 Change in roughness for each deposition method with increasing deposition cycles

Deposition method	RMS roughness
Bare Silicon	0.32
PS 5	1.73
PS 7	2.54
PS 9	2.68
PS 12	2.99
PS 15	3.47
PS 18	3.31
PS 21	3.90
PS 24	4.48
IS 1	1.01
IS 2	1.07
IS 3	1.11
IS 7	1.57
CD	5.51

suspension used, an increasing density of impurities was observed with increasing deposition cycles. Such an increase was not observed for the case of deposits formed when suspensions are drop-cast onto to substrates rotating at high speed [41]. This increase in impurities was likely due to the painting process allowing time for any carbonaceous impurities in the suspension to deposit on the substrate via electrostatic interactions with the amine-functionalized surface. These impurities were responsible for a consistent increase in the root-mean-square (RMS) roughness, with increasing deposition cycles (Table 1). Therefore, although height analysis of AFM images indicated that each deposition cycle resulted in the deposition of low densities of unbundled SWNTs, the RMS roughness increased from 1.73 to 4.48 for 5–24 deposition cycles, respectively. The RMS roughness for the PS method was found to be consistently higher than that for the IS method. However, as the CD method allowed time for complete drying, it resulted in the highest observed RMS roughness of the three deposition methods evaluated.

The painting method clearly results in the deposition of greater densities of unwanted carbonaceous impurities. However, an advantage of this method over drop casting is that the uniform suspension layer formed before spinning at high speeds allowed a homogenous distribution of SWNT lengths throughout the deposit. As the PS method starts with a thin homogeneous suspension layer, no changes in length as a function of distance from the center of rotation were observed. Alternatively, when SWNT suspension is drop-cast onto a substrate that is rotating at a high spin-rate, the magnitude of centripetal force acting on each SWNT increases with its length [41]. This results in length gradients throughout the film. Therefore, despite its requirement for improved purity in deposition suspensions, the PS method has an increased potential for the reproducible formation of well-defined thin films.

The PS method has the additional advantage of reducing suspension requirements to 0.02 mL/cm^2 substrate. This low volume of suspension minimizes any edge effects (caused by solvent pooling at the edge of the wafer until a bead is large enough to leave the edge). In addition, as there is a short interval (<5 s) between suspension deposition and initiating high-speed sample rotation, the amount of bundling that occurs during the drying process is minimized. Thus, the deposition of unbundled SWNTs occurs after a laminar fluid flow phase in the rapidly thinning aqueous layer, as in previous studies using a manual drying technique [27, 30]. This allows these liquid-deposited networks to behave as semiconductive thin-films at sufficiently low network densities.

IS method

For the IS method, a 10–12 min incubation period facilitated the formation of 2-D clusters of SWNTs (Fig. 3a). These clusters, which were observed to have a thickness consistent with one layer of SWNTs, could be described as <2 nm-high low-density groups of parallel SWNTs. At incubation times greater than 12 min, the side-by-side growth of bundles was augmented with 3-D growth. For example, when a single deposition with a 25 min incubation time was used, the height of the bundles was significantly greater (Fig. 3b). Therefore, the growth pattern of these 2- and 3-D clusters appears to follow a nucleation and growth mechanism, with the initially deposited low-density arrays of SWNTs acting as seed crystals for the deposition of additional nanotubes. As deposition, this process occurs only at the substrate/suspension/air interface, this process was repeated with a series of successively larger drops of suspension to increase the coverage of the 2-D clusters.

For repeated deposition times of 10 min, the RMS roughness increased at a much slower rate than that observed for the PS methods, from 1.01 to 1.57 over seven deposition cycles. This indicates that while 2-D clusters of aligned SWNTs dominate the deposit, any carbonaceous impurities remaining in the suspension are far less likely to be deposited. This can be explained by a closer examination of the deposition process. The deposition of suspended particles primarily at the substrate/suspension/air interface can be attributed to a "coffee-ring" effect, as described by Deegan and coworkers [33]. In brief, as a drop of a suspension evaporates, the evaporation rate is greater at the edges than at the center of the drop, due to surface area effects. This differential evaporation rate results in capillary flow from the center to the

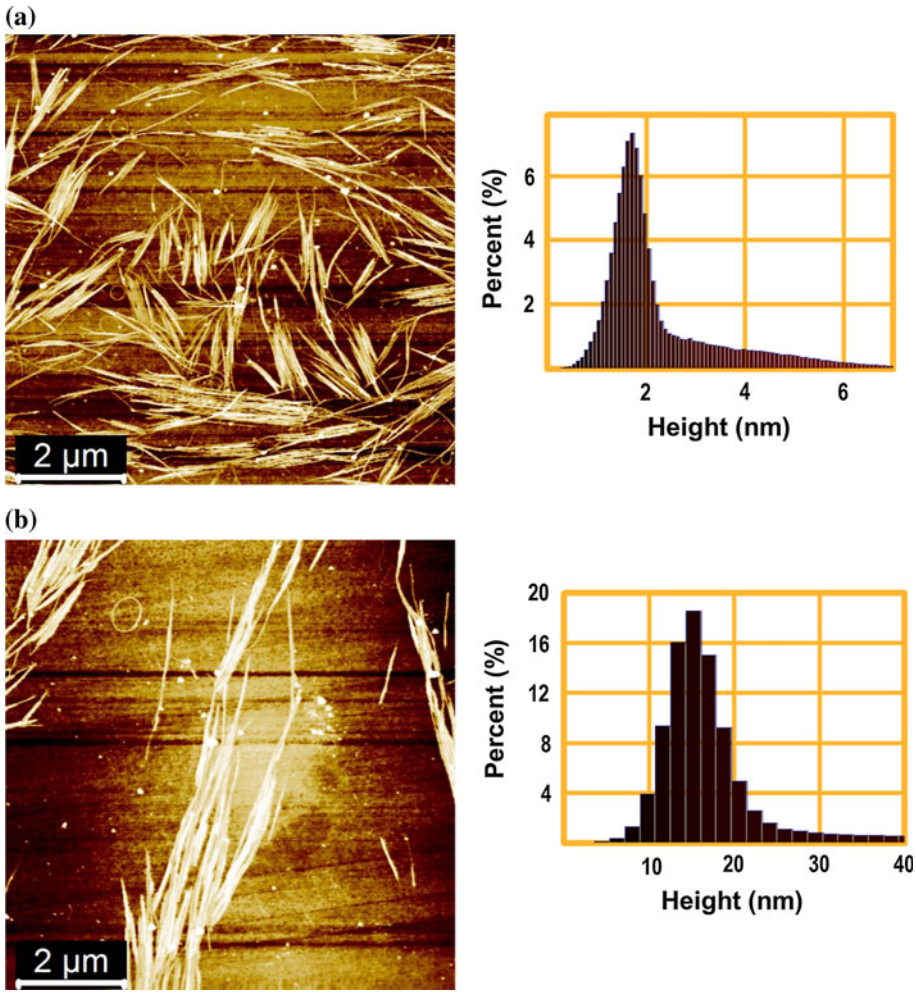

Fig. 3 AFM data of high-aspect ratio SWNTs deposited from the partial evaporation of sessile drops using the IS method: **a** 2-D clusters were formed when incubation times of 10–12 min were used and a height histogram of the *z*-range of every pixel in the image shows an average height of 1.7 nm, indicating that the clusters were composed of a single layer of SWNTs; **b** for an incubation time of 25 min, the 2-D clusters acted as nucleation points for the 3-D growth of SWNT bundles and the average height observed is 16 nm

edges of the drop. As the contact line of the suspension is pinned during the early stages of evaporation, this outbound suspension flow transports particles to the drop's edge, where they deposit as the solution evaporates. A unique power-law equation was proposed to describe the increase in mass at the drop's edge. Subsequent study by Hu and coworkers demonstrated that this solution flow is sufficient to return the particles to the center of the drop, unless the flow-rate is dampened by surfactants that reduce the solution's surface tension, and subsequently, the capillary flow-rate [42].

For the suspensions of high aspect ratio SWNTs used in these studies, the circular evaporation-induced flow of the solution was sufficient to deposit 2-D clusters of SWNTs near the drying line (Fig. 4). This behavior can be attributed to the fact that the high-aspect ratio SWNTs in the deposition suspensions were of sufficient length to be transported to the solvent front by capillary forces, but too massive to return to the center of the suspension with the solvent. Therefore, these high-aspect ratio SWNTs were deposited at the edge of the drop.

The monolayer thickness of these deposits is due to the strong electrostatic interactions between the amine-terminated surface and defects on the nanotubes, as well as the extended π-bonding network of the SWNT sidewalls. In addition, confinement effects due to the thin solution layer at the drop's edge facilitated the deposition process. The interplay between the surface/SWNT electrostatic interactions and the inter-SWNT van der Waals forces are responsible for the 2-D cluster formation dominating at low incubation times. At longer incubation times, inter-SWNT van der Waals forces result in 3-D growth being thermodynamically favored over further nucleation. The disorder in the orientation of the 2-D bundles with respect to one another is likely induced by the spinning process.

CD method

Of the three methods investigated, only the CD method consistently deposited large 3-D aggregates, resulting in dense networks composed of bundles of SWNTs (Fig. 5a). In addition, the extended drying times used in

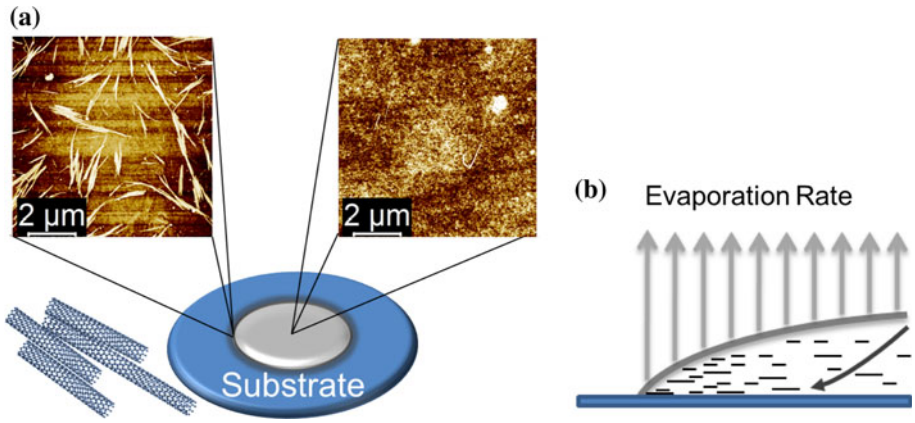

Fig. 4 In the IS deposition method **a** a sessile drop of SWNT suspension is allowed to incubate on the wafer for 10–12 min; **b** this incubation time allows the development of evaporation-driven currents that concentrate the SWNTs at the substrate/suspension/air interface, as the contact line is pinned for short evaporation times. After the wafer is spun at 1200 rpm for 12 s, the process was repeated with the addition of increasingly larger drops of suspension

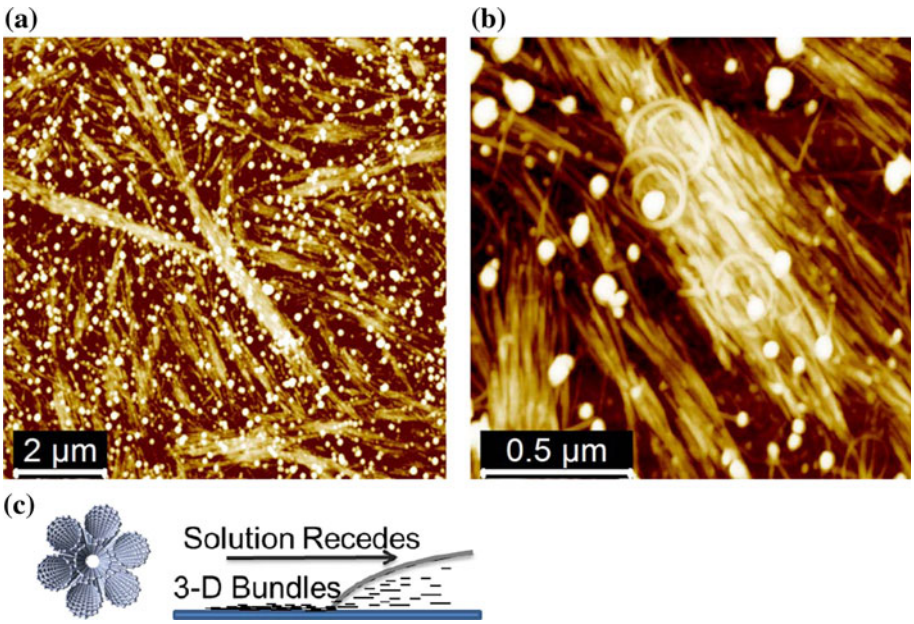

Fig. 5 AFM images of networks deposited using the CD method show that **a** a small degree of inter-bundle alignment is evident on a large scale; **b** the SWNTs form large bundles due to alignment and condensation driven by currents caused by evaporative forces in the suspension; **c** for extended drying times, 3-D bundles of SWNTs are deposited at the substrate/suspension/air interface, as the solvent front recedes

this deposition method resulted in a greater degree of inter-SWNT bundle alignment. A greater concentration of carbonaceous impurities is also evident. This was not the case for the PS method due to the rapid deposition process from small volumes of suspension, or the IS method, as these impurities apparently remained trapped in the circular capillary solvent currents utilized to deposit the more massive nanotubes at the suspension's edge. As the suspension is allowed to dry completely in this deposition method, all the impurities remaining in the suspension are deposited onto the SWNT network (Fig. 5b). Therefore, after only one deposition cycle, the CD method had the highest RMS roughness of the three methods investigated.

Effect deposition method on macroscopic electronic transport

PS method

As the PS method uses an increasing number of deposition cycles to build a low-density network, the change in macroscopic conductance with the density of SWNTs can be modeled with percolation theory [43, 44]. When applied to a random array of conducting sticks, Eq. 1 describes the critical density, N_c, above which macroscopic conduction is observed.

$$N_c = \frac{4.236^2}{l^2 * \pi} \quad (1)$$

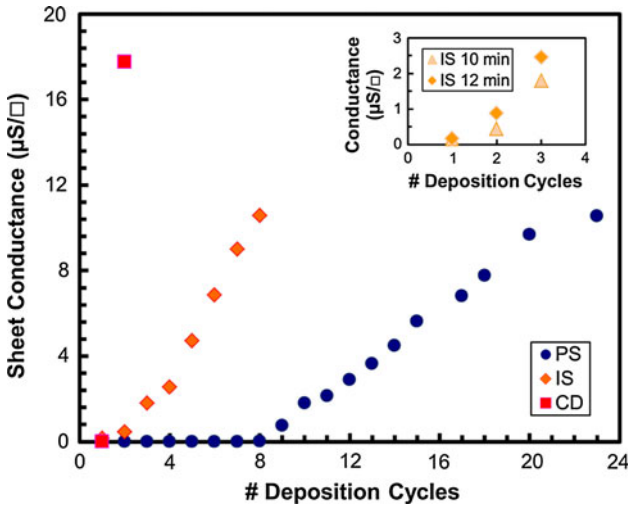

Fig. 6 The PS method allowed the maximum level of control over the sheet conductance of the network, as unbundled, high-aspect ratio SWNTs were deposited with controlled density. Alternatively, the increase in conductivity was greater for the IS and CD methods, in which each deposition cycle deposits increasing densities of 2- and 3-D bundles, respectively

where 4.236^2 is a theoretical constant based on a conducting sticks model [45], l is the average length of the SWNTs in the network, and π represents the ratio of a circle's circumference to its diameter (as an SWNT can have any angle of rotation in the plane of the substrate).

Since an average length of 1.5 ± 0.4 μm was observed for the SWNTs, N_c is expected to be 2.5 SWNT/μm^2. As a low density of SWNTs is deposited in each deposition cycle, eight repetitions were required to achieve this density and observe macroscopic conduction (Fig. 6). The slowest increase in the slope of the conductance versus number of deposition cycles curve was observed for the PS method, as it builds up SWNT networks by repeatedly depositing ultra-low densities of unbundled SWNTs until the desired network density is reached.

IS method

The magnitude of the conductance for the IS method was intermediate with respect to the other two deposition methods. The macroscopic conductance observed indicates that although SWNT clusters were deposited preferentially at the drop's edge, repeating the process with successively larger volumes of suspension resulted in the formation of macroscopic networks of 2-D clusters. Therefore, the IS method allowed the deposition of 2-D clusters of aligned SWNTs over an increasing area as the number of deposition cycles increased.

In addition, when the incubation time was increased from 10 to 12 min (Fig. 6, inset), the slope of the plot of sheet versus number of deposition cycles increased. This indicates that allowing greater time for the nucleation and growth of the SWNT clusters resulted in the deposition of greater densities of nanotubes as repeating the deposition process allowed the capillary flow process that deposited SWNTs to increase the density of 2-D bundles. This indicates that this deposition process can be tuned via both the number of deposition cycles and the incubation times used in each deposition. The IS method, like the PS method, could be repeated until the desired macroscopic electrical properties are achieved, facilitating applications that require conductive and transparent thin-films. Alternatively, on the microscopic scale, such 2-D clusters may have applications in the formation of highly conductive interconnects between electronic device structures.

CD method

Finally, deposits formed using the CD method showed the greatest increase in conductivity, as each deposition cycle deposited large 3-D bundles of SWNTs. In fact, after just two deposition cycles, the sheet conductance far surpassed that of the highest observed conductance for the other two methods. This is due to the deposition of high-densities of 3-D bundles of SWNTs in each deposition cycle. The high conductance of these 3-D bundles makes them a possible route to the formation of highly conductive thin-films that are compatible with flexible substrates.

Effect of deposition method on field-effect transistor performance

PS method

The 2/1 ratio of semiconductive/metallic SWNTs in arc discharge soot [8] allows one to use a FET configuration to obtain a qualitative measure of the degree of bundling induced by each deposition process (Fig. 7). When the gate voltage is scanned from negative to positive, only networks composed of low-densities of unbundled SWNTs behave as semiconductive thin-films. The semiconductive thin-films exhibit a strong dependence of source/drain current on gate voltage, while the metallic thin-films show little change. The semiconductive behavior is consistently observed in the density limit between N_c for the semiconductive and the metallic SWNTs. Thin-films with densities above N_c for the metallic SWNTs, as well as networks composed of bundles of SWNTs, consistently exhibit metallic conduction.

The conductivity of the 2-D networks deposited with the PS method showed a reduction of over two orders of magnitude as the gate voltage was scanned from −4 to 1 V. This behavior is typical of a p-type semiconductor.

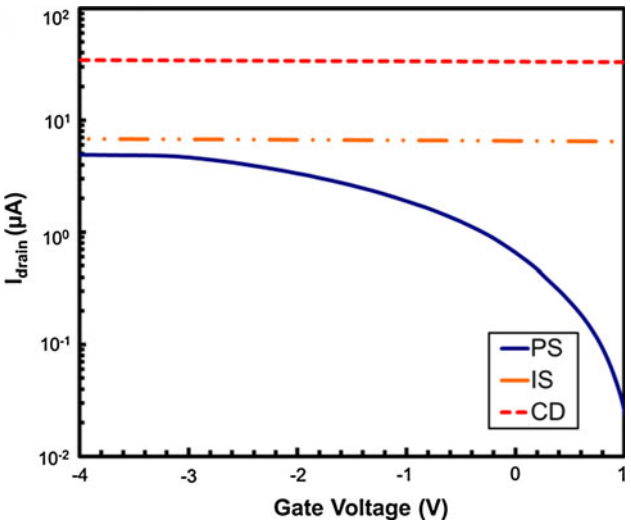

Fig. 7 When tested in a FET configuration, the conductance of the network composed of a low density of unbundled SWNTs changed by several orders of magnitude as the gate voltlage was scanned, while the conductance of the two networks composed of bundles of SWNTs remain comparatively unchanged

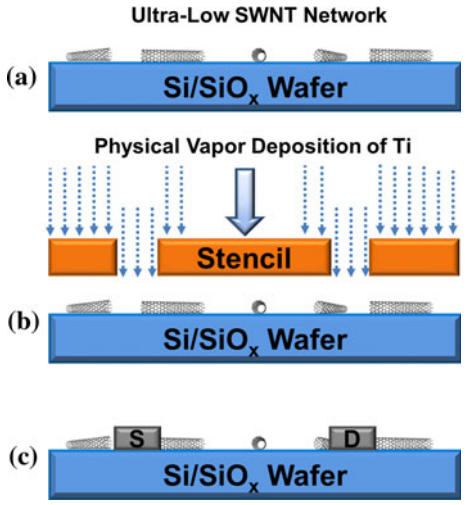

Fig. 8 SWNT network transistor formation: **a** an initial ultra-low density of SWNTs was deposited. Macroscopic conductivity was not observed for these deposits; **b** a stencil mask was used during high-vacuum thermal deposition of Ti; **c** the resulting Ti electrodes have enhanced contacts to the pre-deposited SWNTs, allowing better electrical contacts to the SWNTs deposited during the formation of the conducting network

However, the networks deposited using the IS and CD methods show little change in conductivity in this same voltage range. This difference in macroscopic transport is caused by the presence of 2-D clusters and 3-D bundles of SWNTs in networks deposited using the IS and CD methods, respectively. This behavior results from metallic SWNTs, which remain unaffected by the gate voltage, acting as current pathways.

Previous reports have shown that the contact resistance at the metal/SWNT interface plays an important role in FET performance [46, 47]. An additional study has demonstrated that the contacts to both semiconductive and metallic SWNTs can be optimized by a local voltage pulse applied through a conducting AFM probe [48]. Under ideal conditions, FET devices composed of liquid deposited networks of unbundled SWNTs have exhibited on/off ratios of $>10^6$, if the contact resistance to the metal electrodes was minimized [49]. Therefore, a new approach to device fabrication was employed (Fig. 8) to understand the effect of the number of deposition cycles on the on/off ratio of FET devices. An ultra-low density of SWNTs (below the percolation threshold for semiconductive SWNTs) was deposited through one deposition cycle from a suspension with an SWNT concentration of 0.1 mg/mL. The macroscopic conductivity was not observed for these layers. Then, thermal deposition of Ti through a stencil was employed to form source and drain electrodes spaced 1 cm apart.

While macroscopic conductance was not observed for these samples, the ultra-low density of pre-deposited SWNTs provided a foundation for the enhanced electrical conductivity to SWNTs that were deposited subsequently; a small portion of the pre-deposited SWNTs remained partially covered, extending into the source/drain channel, allowing low-resistance SWNT-SWNT contacts to dominate between the Ti electrodes. This resulted in the reduction of the SWNT/Ti interfacial Schottky barrier typically observed for such devices. Consequently, an enhanced conductivity was observed throughout a wide range of deposition cycles when SWNT suspensions of 0.02 mg/mL were subsequently employed to deposit networks exhibiting tunable macroscopic conductivity as subsequently deposited SWNTs contacted the pre-deposited SWNTs near the SWNT/Ti electrode interface.

In a standard FET characterization setup, 0.5 V was applied between the source and the drain electrodes while the gate voltage was scanned between ±5 V. The on/off ratio increased from 1.2×10^4 to 2.0×10^4 for 1–3 deposition cycles (Fig. 9). Then, the maximum on/off ratio, 2.5×10^5, was observed after four deposition cycles. Therefore, four deposition cycles mark the point at which the ratio of the number of semiconductive/metallic pathways reaches a maximum. Additional deposition cycles result in an increase of the number of metallic pathways. As the conductivity of these metallic pathways is not strongly affected by the gate bias, the on- and off-state currents begin to increase, with a concurrent decrease in the on/off ratio.

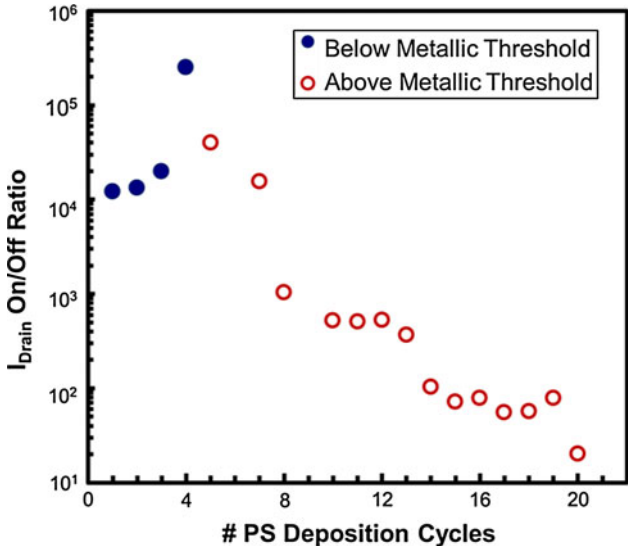

Fig. 9 As the gate voltage was scanned between ±5 V (0.5 V was applied between the source and drain electrodes), increasing the number of deposition cycles permitted on/off ratio to be tuned to a maximum of 2.5×10^5 for four deposition cycles. Additional deposition cycles resulted in the formation of additional metallic pathways, reducing device performance

IS and CD methods

The IS and CD networks showed little change in the conductivity upon exposure to a gate bias (Fig. 7). This is expected because of the observance of high densities of 2-D and 3-D clusters for networks deposited using the IS and CD methods, respectively. The presence of a single metallic SWNT in a cluster renders it a metallic conductor. This highlights the importance of the development of methods for obtaining strict density control during the formation of SWNT networks.

Conclusion

Three spin-casting techniques have been employed to deposit semiconductive and metallic SWNT networks having tunable electrical transport. The PS method provides a high level of density control during the deposition of 2-D networks of unbundled, high-aspect ratio SWNTs. The conductivity of these networks can be tuned via changes in the density of deposition suspensions and/or the number of deposition cycles. Most of the previously reported liquid deposition techniques allow bundle formation during the drying stage. However, the PS method greatly reduces this effect by first coating the substrate with a thin layer of a suspension of high-aspect ratio SWNTs, reducing suspension use to 0.02 mL/cm^2 of substrate coated. Next, high-speed sample rotation is employed to effect laminar drying of the substrate, resulting in the deposition of low densities of unbundled SWNTs. A major advantage of this method is that these networks can be tuned from semiconductive to metallic by simply increasing the number of deposition cycles. When tested in an FET configuration, these networks consistently behaved as thin-film semiconductors, reaching an on/off ratio of 10^5, indicating that the low-density networks of unbundled SWNTs were formed over a large area. The rate of the increase in conductance for each deposition method varied in the order PS < IS < CD.

In the IS method, 2-D networks, composed of clusters of side-by-side SWNTs, were formed by allowing an incubation time of 10–12 min before the application of centrifugal force. This incubation time allows the formation of circular evaporation-induced currents that deposit high-aspect ratio SWNTs at the drop's edge. This process was repeated with a series of successively larger drops of suspension to grow a 2-D thin-film of clusters of SWNTs with a height consistent with a single layer of nanotubes. As macroscopic conductivity in these networks is supported by 2-D bundles of SWNTs, these networks have metallic conduction. The ability to deposit 2-D clusters of aligned SWNTs provides a route to the formation of electronic device structures that require higher current drive than possible with an individual SWNT.

In the CD method, 3-D networks with high-densities of bundled SWNTs were formed via an evaporation method. The conductance of these networks is also tunable by repeating the deposition process. Semiconductor characterization experiments showed that these highly conductive networks little response to an external gate bias. As these networks show the greatest increase in conductance per deposition cycle and are composed of SWNT bundles, they will likely have applications in device structures that require highly conductive, flexible electronic materials.

Acknowledgement The authors gratefully acknowledge the financial support from the National Science Foundation through NSF Grant DMR-0906564.

References

1. Lefebvre J, Antonov RD, Radosavljevic M, Lynch JF, Llaguno M, Johnson AT (2000) Carbon 38:1745
2. Tans SJ, Verschueren ARM, Dekker C (1998) Nature 393:49
3. Rafii-Tabar H (ed) (2008) Computational physics of carbon nanotubes. Cambridge University Press, Cambridge
4. Appenzeller J, Martel R, Derycke V et al (2002) Microelectron Eng 64:391
5. Chen J, Klinke C, Afzali A, Avouris P (2005) Appl Phys Lett 86:123108
6. Terrones M (2003) Annu Rev Mater Res 33:419
7. Dai H (2002) Acc Chem Res 35:1035
8. Dai LM, Soundarrajan P, Kim T (2002) Pure Appl Chem 74:1753

9. Pengfei QF, Vermesh O, Grecu M et al (2003) Nano Lett 3:347
10. Zhang Q, Vichchulada P, Cauble MA, Lay MD (2009) J Mater Sci. 44:1206. doi:10.1007/s10853-009-3256-7
11. Saran N, Parikh K, Suh DS, Munoz E, Kolla H, Manohar SK (2004) J Am Chem Soc 126:4462
12. LeMieux MC, Roberts M, Barman S, Jin YW, Kim JM, Bao ZN (2008) Science 321:101. doi:10.1126/science.1156588
13. Park YT, Ham AY, Grunlan JC (2011) J Mater Chem 21:363. doi:10.1039/c0jm02524k
14. Xiao GZ, Tao Y, Lu JP, Zhang ZY, Kingston D (2011) J Mater Sci 46:3399. doi:10.1007/s10853-010-5228-3
15. Jiao LY, Xian XJ, Wu ZY, Zhang J, Liu ZF (2009) Nano Lett 9:205. doi:10.1021/nl802779t
16. Pushparaj VL, Shaijumon MM, Kumar A et al (2007) Proc Natl Acad Sci USA 104:13574
17. Masarapu C, Zeng HF, Hung KH, Wei B (2009) Acs Nano 3:2199. doi:10.1021/nn900500n
18. Vairavapandian D, Vichchulada P, Lay MD (2008) Anal Chim Acta 626:119. doi:10.1016/j.aca.2008.07.052
19. Siqueira JR, Werner CF, Backer M et al (2009) J Phys Chem C 113:14765. doi:10.1021/jp904777t
20. Vichchulada P, Shim J, Lay MD (2008) J Phys Chem C 112: 19186
21. Bekyarova E, Itkis ME, Cabrera N et al (2005) J Am Chem Soc 127:5990. doi:10.1021/ja0431531
22. ZC Wu, Chen ZH, Du X et al (2004) Science 305:1273
23. Rowell MW, Topinka MA, McGehee MD et al (2006) Appl Phys Lett 88:233506. doi:23350610.1063/1.2209887
24. Jung MS, Hyeon-Lee JY, Lee JH, Park JJ, Jung IS, Kim JM (2008) Adv Funct Mater 18:449. doi:10.1002/adfm.200700448
25. Jang EY, Kang TJ, HW Im, Kim DW, Kim YH (2008) Small 4:2255. doi:10.1002/smll.200800600
26. Gruner G (2006) J Mater Chem 16:3533
27. Zhang Q, Vichchulada P, Lay MD (2010) Phys Status Solidi A 207:734. doi:10.1002/pssa.200723106
28. Park JU, Meitl MA, Hur SH et al (2006) Angew Chem Int Ed 45:581. doi:10.1002/anie.200501799
29. Eda G, Fanchini G, Kanwal A, Chhowalla M (2008) J Appl Phys 103:093118. doi:10.1063/1.2919164
30. Vichchulada P, Zhang Q, Duncan A, Lay MD (2010) ACS Appl Mater Interfaces 2:467. doi:10.1021/am900706p
31. Chen RJ, Bangsaruntip S, Drouvalakis KA et al (2003) Proc Natl Acad Sci USA 100:4984
32. Shim J, Vichchulada P, Zhang Q, Lay MD (2010) J Phys Chem C 114:652. doi:10.1021/jp9086738
33. Deegan RD, Bakajin O, Dupont TF, Huber G, Nagel SR, Witten TA (1997) Nature 389:827
34. Lian YF, Maeda Y, Wakahara T et al (2003) J Phys Chem B 107:12082. doi:10.1021/jp035118r
35. Maeda Y, Kimura S, Kanda M et al (2005) J Am Chem Soc 127:10287. doi:10.1021/ja051774o
36. Zhou XJ, Park JY, Huang SM, Liu J, McEuen PL (2005) Phys Rev Lett 95:146805
37. Zhou O, Shimoda H, Gao B, Oh S, Fleming L, Yue G (2002) Acc Chem Res 35:1045
38. Tseng YC, Phoa K, Carlton D, Bokor J (2006) Nano Lett 6:1364
39. Vichchulada P, Vairavapandian D, Lay MD (2009) Phys Status Solidi-RRL 3:31. doi:10.1002/pssr.200802236
40. Vichchulada P, Zhang Q, Lay MD (2007) Analyst 132:719. doi:10.1039/b618824a
41. Zhang Q, Vichchulada P, Lay MD (2010) J Phys Chem C 114:16292. doi:10.1021/jp105884e
42. Hu H, Larson RG (2006) J Phys Chem B 110:7090. doi:10.1021/jp0609232
43. Stauffer D (1985) J Phys A 18:1827
44. Obukhov SP (1988) J Phys A 21:3975
45. Pike GE, Seager CH (1974) Phys Rev B 10:1421
46. Heinze S, Tersoff J, Martel R, Derycke V, Appenzeller J, Avouris P (2002) Phys Rev Lett 89:106801. doi:10.1103/PhysRevLett.89.106801
47. Lee CW, Zhang K, Tantang H et al (2007) Appl Phys Lett 91:103515. doi:10.1063/1.2772181
48. Nirmalraj PN, Boland JJ (2010) Acs Nano 4:3801. doi:10.1021/nn100432f
49. Lee CW, Weng C-H, Wei L et al (2008) J Phys Chem C 112: 12089. doi:10.1021/jp805434d